Article:
Hesas, RH, Baei, MS, Rostami, H et al. (2 more authors) (2019) An investigation on the capability of magnetically separable Fe_3O_4/mordenite zeolite for refinery oily wastewater purification. Journal of Environmental Management, 241. pp. 525-534. ISSN 1095-8630

https://doi.org/10.1016/j.jenvman.2018.09.005

An investigation on the capability of magnetically separable Fe_3O_4/mordenite zeolite for refinery oily wastewater purification

Roozbeh Hoseinzadeh Hesas[1], Mazyar Sharifzadeh Baei[1, †], Hadi Rostami[1], Jabbar Gardy[2], Ali Hassanpour[2]

[1] Department of Chemical Engineering, Ayatollah Amoli Branch, Islamic Azad University, Amol, Iran

[2] School of Chemical and Process Engineering, University of Leeds, Leeds, LS2 9JT, UK

[†] E-mail: m.sharifzadeh@iauamol.ac.ir

Abstract

Damage to the water resources and environment as a consequence of oil production and use of fossil fuels, has increased the need for applying various technologies and developing effective materials to remove oil contaminates from oily wastewaters resources. One of the challenges for an economic industrial wastewater treatment is separation and reusability of developed materials. Development of magnetic materials could potentially facilitate easier and more economic separation of purifying agents. Therefore, herein we have synthesised an efficient and easily recyclable Fe_3O_4/mordenite zeolite using a hydrothermal process to investigate its purification capability for wastewater from Kermanshah oil refinery. The synthesised Fe_3O_4/mordenite zeolite was characterised using XRD, FTIR, SEM, EDX, XRF and BET analysis. XRD result showed that the synthesised Fe_3O_4/mordenite zeolite comprised sodium aluminium silicate hydrate phase [01-072-7919, $Na_8(Al_6Si_{30}O_{72})(H_2O)_{9.04}$] and cubic iron oxide phase [04-013-9808, Fe_3O_4]. Response Surface Method (RSM) combined with Central Composite Design (CCD) was used to identify the optimum operation parameters of the pollutant removal process. The effect of pH, contact time and Fe_3O_4/mordenite zeolite amount on the Chemical Oxygen Demand (COD), Biochemical Oxygen Demand (BOD) and Nephelometric Turbidity Unit (NTU) were investigated. It was found that pH was the most significant factor influencing COD and BOD removal but the quantity of Fe_3O_4/mordenite zeolite was the most influential factor on turbidity removal capacity. The optimum removal process conditions were identified to be pH of 7.81, contact time of 15.8 min and Fe_3O_4/mordenite zeolite amount of 0.52 wt/wt%. The results show that the regenerated Fe_3O_4/mordenite zeolite can be reused for five consecutive cycles in purification of petroleum wastes.

Keywords: Oily wastewater purification; Oil refinery wastewater treatment; Fe_3O_4/mordenite zeolite; COD; BOD; NTU.

Research highlights

- Fe_3O_4/mordenite zeolite particles was synthesised and characterised.
- We examined the capability of Fe_3O_4/mordenite zeolite for oily wastewater purification.
- The response surface methodology was used to optimise the removal parameters.
- The magnetic particles can be re-used multiple times without loss of activity.

Graphical abstract

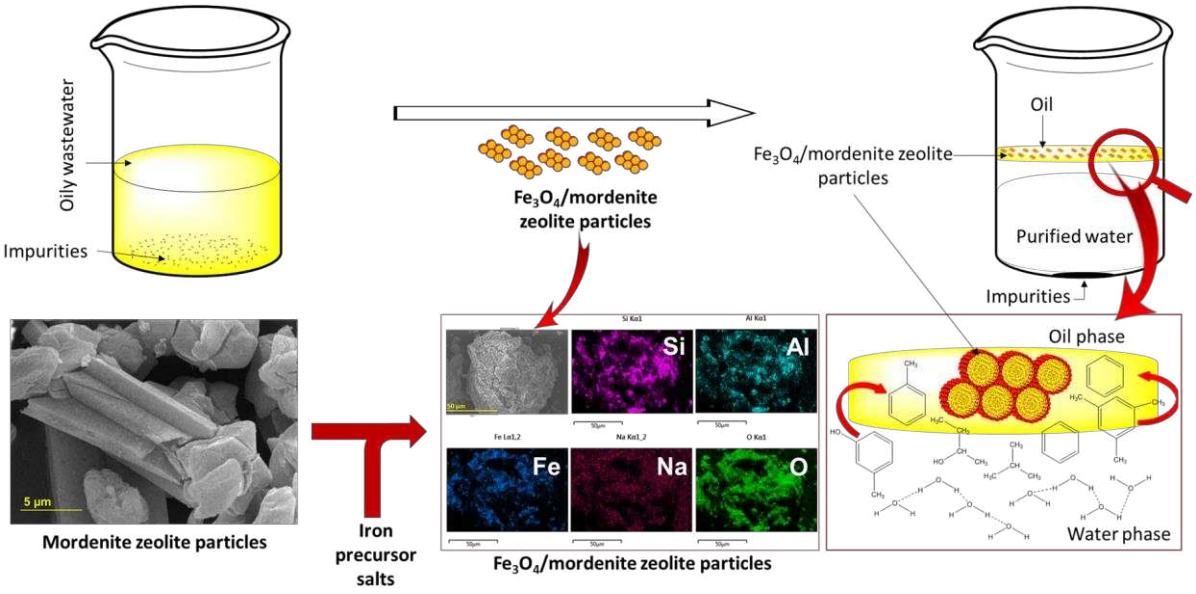

1. Introduction

In the past few decades, water pollution has become a serious environmental concern [1, 2]. Among water pollutants, oil is found in both industrial wastewaters and drinking water reservoirs sourcing from different sectors, including food processing, transportation and the petroleum and petrochemical industries [3-7]. Current crude oil yield is ~84 million barrels per day but about 0.4-1.6 times of crude oil production is discharged as petroleum wastewater [8]. As a result, managing the water source in terms of optimising water consumption and introducing new technologies for water recycling has attracted strong interest within the petroleum and petrochemical industries. Generally, the refinery waste contains inorganic materials such as Mg^{2+}, Ca^{2+}, S^{2-}, Cl^{-} and SO_4^{2-} as well as emulsion oil and petroleum, cresols, sulfides, phenols, ammonia and cyanides [9-11].

Mineral and waste types adsorbents such as carbon nanotubes [12-14], clay/anthracite composite [15], wool fibers [16], bentonite [17], carbonized rice husk [18, 19] and amine-functional agricultural wastes [20] have been used to remove oil droplets from oily wastewater. There are several techniques to separate oil from water (demulsification) such as flotation [21-23], chemical destabilization [24], membrane separation [25-27], electrocoagulation [28, 29] and adsorption have some advantages such as high COD removal, non-usage of chemical additives and compactness of the treatment units [30-32]. Adsorption is one of the most common methods for demulsification among these techniques and zeolite adsorbent has certain advantages over other conventional methods for industrial wastewater treatment [33]. For oil pollutions removal, the absorption is controlled by van der Waals forces, oil viscosity, pore morphology and the hydrophobic interaction between oils and the absorbents [34, 35].

Zeolites are hydrated aluminium silicate crystals that have alkaline and alkaline earth metal cations with infinite structure. The properties of these compounds include their cation exchange ability and process reversibility without any major change in their molecular structure. The natural zeolites have a negative charge on their surfaces and therefore have the ability to exchange cations [36]. Zeolites have been used as molecular sieves [37], gas storage [38], catalyst [39-42], preparation and modification of soil [43], removing odour [44], and absorption of heavy metals [45, 46].

The primary purification of oil refinery wastewaters can be obtained by combining physical and physicochemical separations of free oil and suspended solid particles and colloidal materials. However, these processes cannot remove emulsion or petroleum oil which is considered in the secondary purification step. After primary purification, refinery oily

wastewaters usually contain aromatic hydrocarbons and compounds such as ethyl benzene, toluene, benzene and 1-ethyl methyl benzene. In addition, separation and recycling of adsorbent materials are two other major challenges for usage in industrial applications. Therefore, we investigate the capability of easily separable Fe_3O_4/mordenite zeolite adsorbent for purification of refinery oily wastewater treatment. The decontamination experiments and optimisation were performed by investigating the effects of pH, contact time and Fe_3O_4/mordenite zeolite amount on efficacy of refinery oily wastewater purification. The regeneration and reusability of synthesised Fe_3O_4/mordenite zeolite in purification of refinery oil wastewaters were also studied.

2. Material and methods

2.1. Synthesis of Fe_3O_4/mordenite zeolite

Mordenite zeolite was synthesised as follows: Aluminosilicate milky gel was made by mixing specific amounts of sodium silicate (Na_2SiO_3, Sigma-Aldrich) and sodium aluminate ($NaAlO_2$, Sigma-Aldrich) in deionised water. The proportion of materials and the coefficients of the above compounds for the gel preparation are specified based on the desired zeolite formula (10 Na_2O - 1.0 Al_2O_3 - 30 SiO_2 - 780 H_2O). To prepare the gel, a definite mass basis was contemplated and then the appropriate amounts of every element (Si, Al, Na, O and H) were calculated from molar and mass bases. A small amount of sodium aluminate powder was added to deionised water and then mixed until it complete dissolved after several hours. The resulting solution was added to another solution, which was prepared from the rapid addition of sodium silicate to deionised water. The obtained milky gel was then mixed for 30 min at 600 RPM to homogenise the gel. The prepared gel was poured into an autoclave and then properly sealed and heated for 24 h at 170 °C. The produced material was filtered using Buchner funnel and then washed with deionised water until the pH changed to below 10 followed by aging at room temperature for 30 min. The synthesised zeolite was oven-dried at 100 °C followed by aging at room temperature for several days.

Iron oxide coated zeolite particles were synthesised via co-precipitation of two iron salts under alkaline condition to form reddish-brown to black Fe_3O_4 particle coats on the zeolite particles using the following modified procedures [47, 48]: 3% of iron (III) chloride hexahydrate ($FeCl_3.6H_2O$, Sigma-Aldrich) and 2% of iron (II) chloride tetrahydrate ($FeCl_2.4H_2O$, Sigma-Aldrich) dispersed in 100 ml of deionised water followed by heating at 80 °C with vigorous stirring using a hotplate-magnetic stirrer until the resulting solution turned to an orange colour.

To this, 10 ml of 25% ammonium hydroxide (~30%, NH_4OH, Sigma-Aldrich) was added dropwise into the resulting mixture with continuous stirring. This formed a black solution of Fe_3O_4 particles. The obtained solution was added dropwise into 10 g of synthesised zeolite particles and heated at 80 °C with continuous stirring for 30 min. The synthesised particles, finally, were washed many times with deionised water to remove any residue, followed by being oven-dried at 55 °C for 24 h.

2.2. Characterisation of Fe_3O_4/mordenite zeolite

The XRD patterns of Fe_3O_4/mordenite zeolite particles was obtained using a D8 Bruker's diffractometer by CuKα source for 2θ = 5-70° with step size of 0.035. The surface functionality of the synthesised Fe_3O_4/mordenite zeolite particles was studied using a Nicolet iS10 FT-IR spectrometer over the ranges of 650-4000 cm^{-1}. The particle size, morphology, structure surface and the elemental distributions of the synthesised Fe_3O_4/mordenite zeolite particles were investigated using Hitachi scanning electron microscope fitted with an Oxford INCA energy dispersive X-ray spectroscopy (EDS). The sample was prepared for SEM and SEM-EDS analysis by placing over a carbon tabs on an aluminium stub and coated with iridium to minimise the surface charging of sample. The nitrogen porosimetry was undertaken according to the multipoint nitrogen adsorption-desorption method at 77.3 K using Quantachrome Nova 2200 surface analyser. Prior to the analysis Fe_3O_4/mordenite zeolite sample was degassed at 300 °C for 4 h under a vacuum of 10 mmHg. The BET surface area was determined over the relative pressure range of 0.01-0.3 but the total pore volume and average pore diameters were calculated by applying the Barrett-Joyner-Halenda (BJH) method to the desorption isotherm. The full elemental composition was quantified using the X-ray fluorescence (XRF, ZSX Primus-II, Rigaku) spectrometer. Prior to analysis, a glass disk of Fe_3O_4/mordenite zeolite sample was made using a fusion method; a mixture of lithium borates anhydrous (6.5 g) as a flux and 0.5 g of the sample melted at 1000-1100 °C.

2.3. Removal and reusability studies

A batch system (100 g of sample per batch) was used for the removal experiments. Samples of oily wastewater of the Kermanshah refinery had COD, BOD and turbidity of 5000 ppm, 25000 ppm and 24352 NTU, respectively. In each experiment, pH of solutions was determined and adjusted by 1 M H_2SO_4 or 1 M NaOH solution. After each experiment, the solution and Fe_3O_4/mordenite zeolite were separated by the external magnetic field and prepared for analysis and determination of COD, BOD and turbidity. Each experiment was repeated twice

and the error was found to be below 4%. The SQ300 Merck photometer was used for the determination of COD, BOD and turbidity in the refinery waste. Removal efficacy for COD, BOD and turbidity was calculated using **Eqn. 1**:

$$\% \text{ Removal} = \frac{C_i - C_f}{C_i} \times 100 \qquad \textbf{Eqn.}(\mathbf{1})$$

C_i is initial concentration (mg/L), and C_f is the final concentration (mg/L) of COD, BOD and NTU.

The synthesised Fe_3O_4/mordenite zeolite was re-used in five consecutive cycles at the optimum conditions of pH, contact time and Fe_3O_4/mordenite zeolite amount to study the lifetime of the synthesised Fe_3O_4/mordenite zeolite. After each cycle, deionised water was used to wash the Fe_3O_4/mordenite zeolite particles followed by addition of 0.05 M sodium hydroxide with mixing at 150 RPM for 60 min [49]. The used Fe_3O_4/mordenite zeolite was then dried in an oven at 110 °C for 60 min and was used for the next experimental run.

2.4. Design of experiment

The response surface methodology (RSM) is a statistical technique for sensitivity analysis, which can be used to optimise the process parameters. The parameters for the removal capacity of Fe_3O_4/mordenite zeolite were studied in this work with the standard RSM using a central composite design (CCD) for the experiments. The approach was used to optimise and analyse the effective parameters using a minimum number of experiments [50]. Based on CCD the number of experiments, N, with n variables, involves a 2^n factorial runs with 2n axial runs as well as n_c centre runs (including six replicates for the estimation of experimental) (**Eqn. 2**).

$$N = 2^n + 2n + n_c \qquad \textbf{Eqn.}(\mathbf{2})$$

Hence in this study for variables such as pH (X_1), contact time (X_2) and Fe_3O_4/mordenite zeolite amount (X_3) (together with their codes shown in **Table 1**) 20 experiments would be needed which would include 8 factorial points, 6 axial points and 6 replicates at the centre points.

Table 1. Variables and codes used for the CCD

Variables	Code	-1	0	1
pH	X_1	5	7	9
Contact time (min)	X_2	15	20	25
Amount of Fe_3O_4/mordenite zeolite in 100 g sample (wt/wt%)	X_3	0.4	0.5	0.6

The low and high levels of variables are coded as −1 and +1, respectively. The axial points are placed at (±α, 0, 0), (0, ±α, 0) and (0, 0, ±α). α is the distance of the axial point from centre and in this study was fixed at 1. Variables were labelled as follows: PH (7 to 9) (X_1), contact time (15 to 25 min) (X_2), and Fe_3O_4/mordenite zeolite amount (0.4 to 0.6 g) (X_3), while the removal percentages of COD (Y_1), BOD (Y_2) and turbidity (Y_3) were regarded as the process responses. It was then assumed that the process responses (Y) are affected by the interaction between the three variables following a quadratic equation as given by (**Eqn. 3**) [51].

$$Y = b_0 + \sum_{i=1}^{n} b_i x_i + \sum_{i=1}^{n} bii\, x_{ii}^2 + \sum_{i=1}^{n-1} \sum_{j=i+1}^{n} b_{ij}\, x_i x_j \qquad \textbf{Eqn. (3)}$$

In the above equation for n number of variables, X_i to X_j are the coded variables, b_0 is a constant, b_i is coefficient for the linear term, b_{ii} is the quadratic coefficient and b_{ij} is coefficient for the interaction. The Design Expert® software [51] was used to analyse the regression, variance and the response surfaces.

3. Results and discussion

3.1. Characterisation of Fe_3O_4/mordenite zeolite particles

Figure 1 presents the powder XRD profile of Fe_3O_4/mordenite zeolite particles matched with sodium aluminium silicate hydrate phase [01-072-7919, $Na_8(Al_6Si_{30}O_{72})(H_2O)_{9.04}$] and cubic iron oxide phase [04-013-9808, Fe_3O_4]. The main diffraction peaks observed at 2θ values of 9.9, 11.2, 22.3 and 22.7° corresponded to the (020), (200), (330) and (240) reflections for the monoclinic structure of zeolite, respectively. However, for the Fe_3O_4 phase a common set of reflections at 2θ values of 30, 35.6, 37, 43.2, 57.1 and 62.8° were assigned to the (220), (311), (222), (400), (511) and (440) planes, respectively.

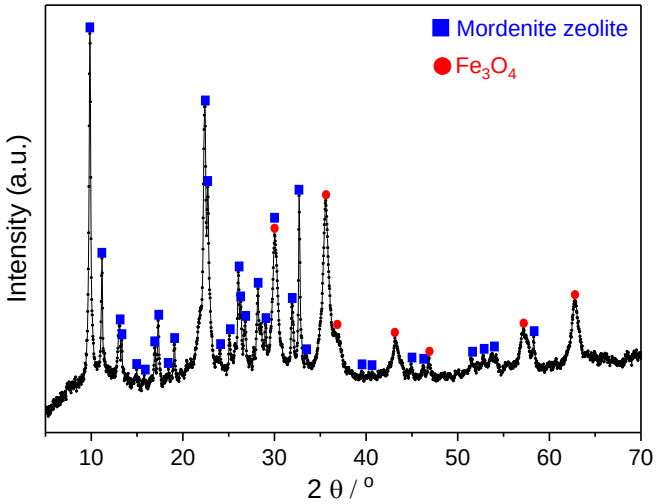

Figure 1. Powder XRD pattern of Fe_3O_4/mordenite zeolite

Figure 2 shows an FTIR spectrum of the Fe_3O_4/mordenite zeolite. The broad peak around 3300 cm^{-1} was related to the stretching vibrations of hydroxyl groups of the zeolite structure [52]. The peak at 1641 cm^{-1} was attributed to the H-O-H symmetric vibration of water molecules in the Fe_3O_4/mordenite zeolite. A strong peak at 1018 cm^{-1} was denoted to an internal asymmetric stretch vibration of M-O-M (where M donates Si, Al or Fe) [40]. The band at 792 cm^{-1} was ascribed to an external asymmetric stretch vibration of M-O-M bending from the SiO_4 or AlO_4 structure [53]. Finally, the bands at 1437 and 626 cm^{-1} were assigned to Fe-O bending and Fe-O stretching vibration, respectively, from the magnetite phase [47].

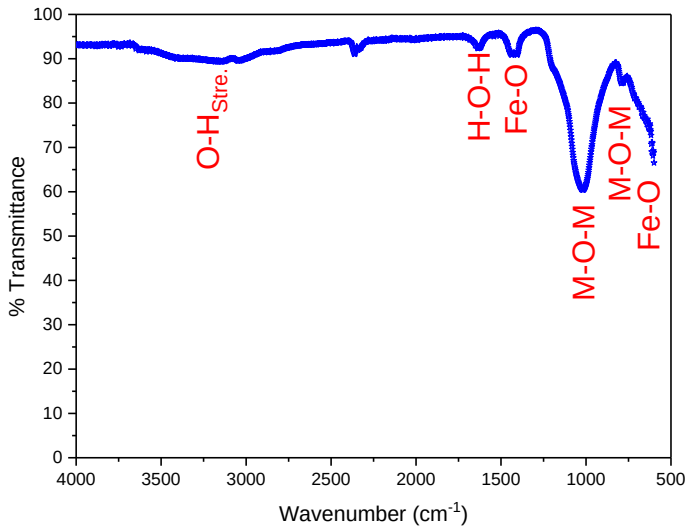

Figure 2. FTIR spectrum of Fe_3O_4/mordenite zeolite

SEM images of the Fe_3O_4/mordenite zeolite at different magnifications are presented in **Figure 3**. It can be observed that the Fe_3O_4 nanoparticles aggregate to each other to form a bigger cluster. The SEM micrographs also consisted mainly of multilayers with a number of pores [53].

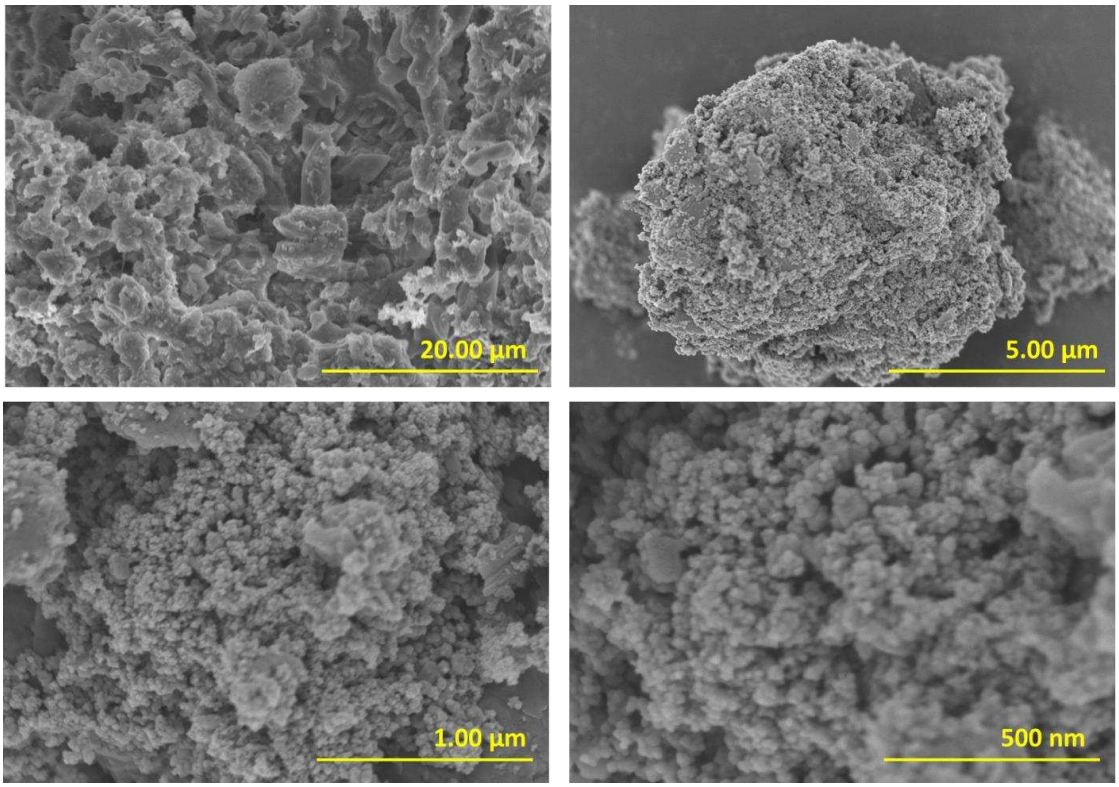

Figure 3. SEM images of Fe_3O_4/mordenite zeolite

The SEM-EDS analysis was used to further explore the existence of iron oxide in Fe_3O_4/mordenite zeolite particles. The corresponding SEM-EDS and EDS-mapping (**Figure 4**) confirm that the synthesised material consist of Si, Fe, Al, O and Na elements and that the Fe element is evenly distributed throughout the elemental mapping. This confirms the successful modification of mordenite zeolite crystals with Fe_3O_4 nanoparticles.

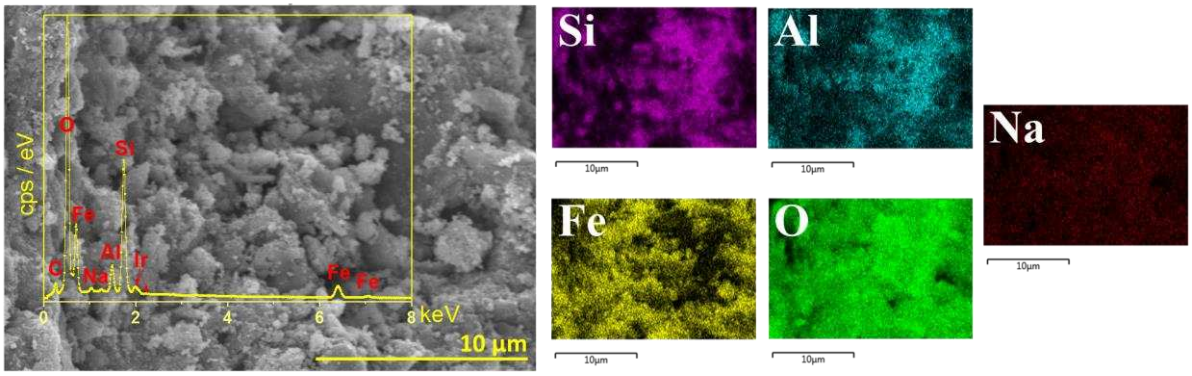

Figure 4. EDS-mapping of Fe_3O_4/mordenite zeolite

Surface area significantly affect the activity of Fe_3O_4/mordenite zeolite for removal processes. Large surface area facilitates easy contact of the molecules on the synthesised Fe_3O_4/mordenite zeolite surface. The texture properties and bulk analysis (obtained from XRF) for Fe_3O_4/mordenite zeolite are presented in **Table 2**. The results obtained from XRF analysis confirm that the synthesised material contains 6:1 atomic ratio of Si to Al.

Table 2. Textural properties and bulk analysis of Fe_3O_4/mordenite zeolite.

S_{BET}[a]	D_p[b]	V_p[c]	Bulk analysis (composition in wt%)[d]				
			SiO_2	Al_2O_3	Na_2O	K_2O	Fe_2O_3
37±1	1.9±0.1	0.12	64.49	10.57	1.77	0.26	22.91

[a] S_{BET}: BET internal surface area ($m^2.g^{-1}$), [b] D_p: Mean pore size (nm); [c] V_p: Total pore volume ($cm^3.g^{-1}$). [d] XRF used for quantification of each elements in synthesised Fe_3O_4 modified/ mordenite zeolite.

The N_2 adsorption-desorption isotherms of Fe_3O_4/mordenite zeolite can be classified as Type IV with one hysteresis loop at a relative pressure range of 0.4-0.983 (**Figure 5**) and suggests the materials is mesoporous with Type H1 of hysteresis loops [54].

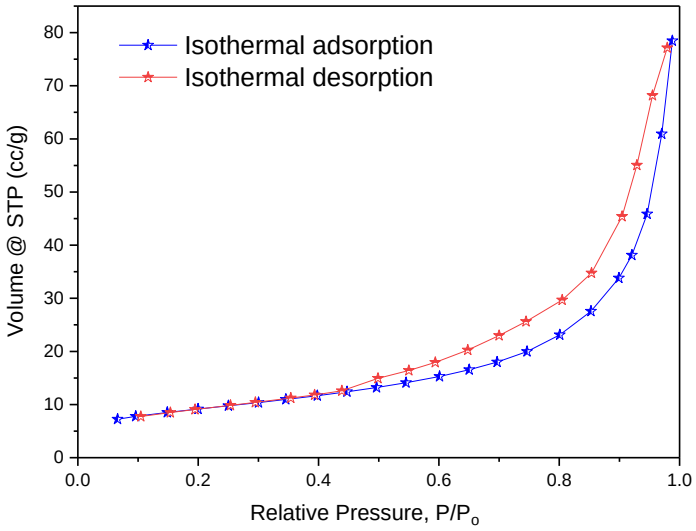

Figure 5. N_2 adsorption-desorption isotherms for Fe_3O_4/mordenite zeolite

3.2. Regression model equation and statistical analysis

The correlation between variables and responses was studied using CCD. **Table 3** shows the three response values obtained from the experimental design matrix. The six runs at pH 7, contact time 20 min and Fe_3O_4/mordenite zeolite amount 0.5 g are the centre points used for the analysis of the experimental error.

Table 3. The design matrix of the experiments and the response values

Run	Type	pH , X_1	Contact time (min), X_2	Adsorbent (Fe_3O_4/mordenite zeolite) amount in 100 g sample (g), X_3	COD Removal (%) , Y1	BOD Removal(%) ,Y_2	Turbidity Removal (%) , Y_3
1	Centre	7	20	0.5	49.82	68.75	76.68
2	Centre	7	20	0.5	49.53	68.45	76.28
3	Factorial	5	25	0.4	35.32	34.27	54.31
4	Factorial	9	15	0.4	20.31	41.15	53.82
5	Axial	5	20	0.5	39.95	37.34	56.64
6	Factorial	5	15	0.4	32.23	31.13	48.78
7	Factorial	9	15	0.6	29.43	51.56	59.93
8	Centre	7	20	0.5	49.21	69.19	76.08
9	Centre	7	20	0.5	49.97	68.85	75.47
10	Axial	7	20	0.6	52.71	74.13	80.12
11	Factorial	9	25	0.4	24.62	47.18	57.75

12	Factorial	5	25	0.6	39.95	44.43	65.01
13	Axial	7	20	0.4	46.56	63.35	72.11
14	Centre	7	20	0.5	49.76	69.32	77.43
15	Axial	9	20	0.5	51.34	71.11	79.02
16	Axial	7	10	0.5	46.45	67.21	70.62
17	Centre	7	20	0.5	50.06	68.13	76.62
18	Factorial	5	15	0.6	38.19	38.18	57.18
19	Factorial	7	25	0.5	28.41	50.17	60.67
20	Factorial	9	25	0.6	31.30	58.72	69.01

For all responses, the quadratic model was selected. The response function of COD, BOD and turbidity removal, was obtained using the regression analysis. The resulting empirical models for COD, BOD and turbidity removal are shown in **Eqns.** (**4**), (**5**) and (**6**), respectively.

$$Y_1 = 49.81 - 4.96x_1 + 1.59x_2 + 3.25x_3 + 0.17x_1x_2 + 0.65x_1x_3 - 0.47x_2x_3 - 16.85x_1^2 - 1.14x_2^2 - 0.40x_3^3 \qquad \textbf{Eqn.}\ (\mathbf{4})$$

$$Y_2 = 68.93 + 6.40x_1 + 2.65x_2 + 4.99x_3 + 0.48x_1x_2 + 0.59x_1x_3 + 0.53\ x_2x_3 - 25.13x_1^2 + 0.003x_2^2 - 0.42x_3^3 \qquad \textbf{Eqn.}\ (\mathbf{5})$$

$$Y_3 = 76.21 + 1.93x_1 + 3.48x_2 + 4.45x_3 - 0.044x_1x_2 - 0.22x_1x_3 + 0.93x_2x_3 - 17.23x_1^2 - 1.07x_2^2 + 0.23x_3^3 \qquad \textbf{Eqn.}\ \mathbf{(6)}$$

The coefficient of the responses for the model were obtained using a multiple regression analysis technique included in the RSM. The correlation coefficient value can be used to evaluate the quality of suggested empirical models. **Figures 6** (**a-c**) shows the predicted response using the **Eqns.** (**4-6**) as compared with the experimental data. It can be seen that the points fall close to the diagonal line, indicating that the empirical models satisfactorily predict the experimental data.

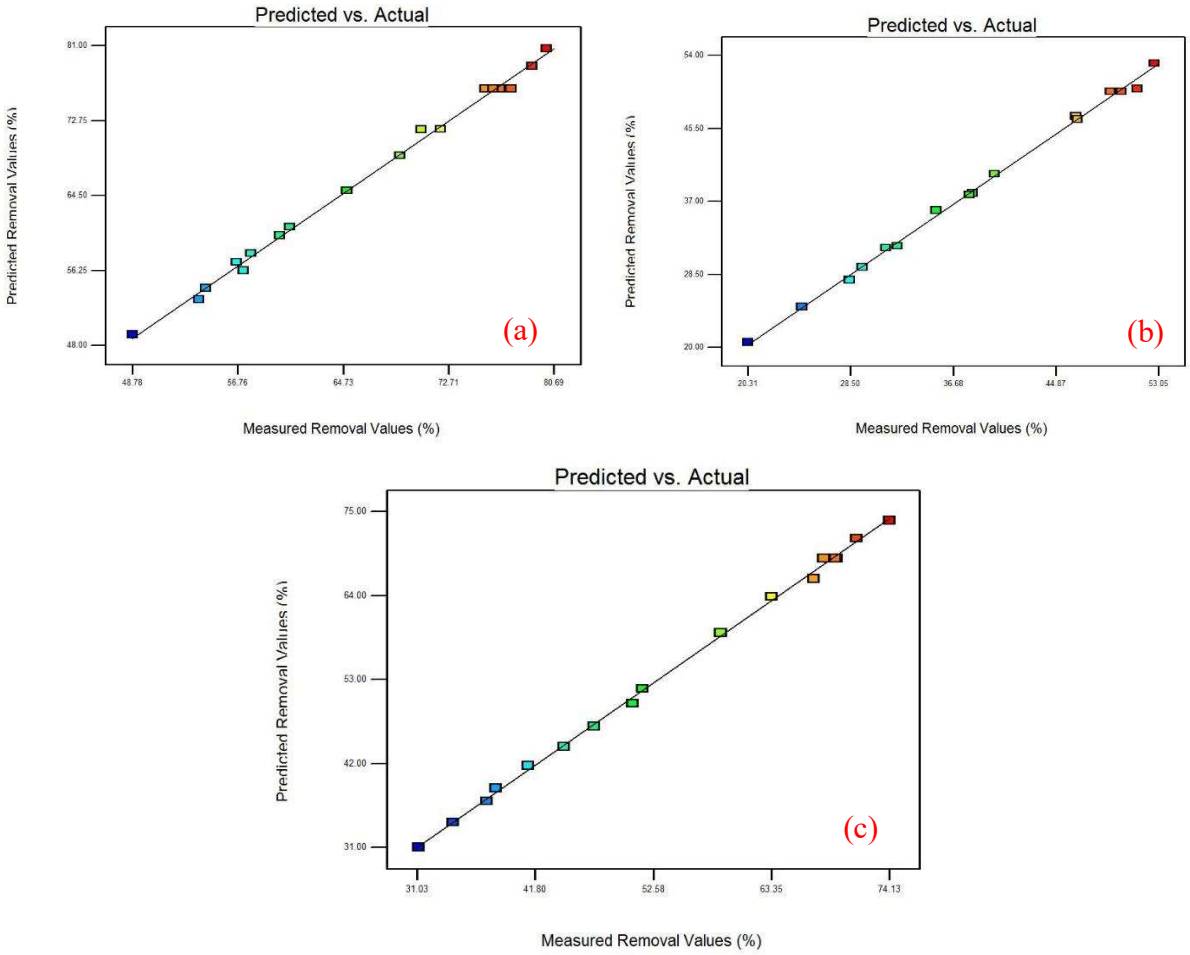

Figure 6. Predicted data vs. experimental value of **(a)** COD removal (%), **(b)** BOD removal (%) and **(c)** turbidity removal (%).

The coefficient of the empirical model (**Eqn. 2**) and their statistical analyses were assessed using the Design Expert® software to identify the experimental variable effects on DOE, BOD and turbidity removal. The F-test analysis of variance was used to evaluate the statistical significance of the quadratic model for pH, contact time and Fe_3O_4/mordenite zeolite amount (**Table 4 a, b and c)**. The statistical analysis shows that these regression are statistically significant at a 99% confidence level. R^2 values for all three responses are close to unity, indicating that all models satisfactorily fit the experimental data.

The p-values of less than 0.05 indicate to significant model term, while the values of higher than 0.1 indicate that model terms are insignificant. For COD removal (Y_1), according to the p-values the pH (X_1), contact time (X_2), Fe_3O_4/mordenite zeolite amount (X_3), interaction effect between pH and adsorbent amount (X_1X_3), interaction effect between contact time and Fe_3O_4/mordenite zeolite amount (X_2X_3), square effect of pH (X_1^2), square effect of contact time

(X_2^2) were significant model terms. Moreover, pH (X_1), contact time (X_2), Fe_3O_4/mordenite zeolite amount (X_3), X_1X_2, X_1X_3, X_2X_3 and X_1^2 in the case of BOD removal (Y_2) and X_1, X_2, X_3, X_2X_3, X_1^2, X_2^2 in the case of turbidity removal were found to be significant model terms.

Table 4. Analysis of variance for response surface quadratic model.

Source	Sum of Squares	Degree of Freedom	Mean of Square	F-Value	p-value	Remarks
(a) COD removal						
Model	1966.86	9	218.54	744.57	< 0.0001	significant
X_1	245.82	1	245.82	837.51	< 0.0001	significant
X_2	25.34	1	25.34	86.35	< 0.0001	significant
X_3	105.89	1	105.89	360.75	< 0.0001	significant
X_1X_2	0.22	1	0.22	0.75	0.4058	Not significant
X_1X_3	3.39	1	3.39	11.56	0.0068	significant
X_2X_3	1.78	1	1.78	6.05	0.0337	significant
X_1^2	780.58	1	780.58	2659.45	< 0.0001	significant
X_2^2	3.56	1	3.56	12.13	0.0059	significant
X_3^3	0.44	1	0.44	1.48	0.2415	Not significant
Residual	2.94	10	0.29	_	_	
Lack of Fit	2.45	5	0.49	5.04	0.0502	Not significant
Pure Error	0.49	5	0.097	_	_	
Cor Total	1969.79	19	_	_	_	
R-Squares	0.9985					
(b) BOD removal						
Model	3956.62	9	439.62	1170.35	< 0.0001	significant
X_1	409.22	1	409.22	1089.40	< 0.0001	significant
X_2	70.12	1	70.12	186.67	< 0.0001	significant
X_3	249.40	1	249.40	663.94	< 0.0001	significant
X_1X_2	1.81	1	1.81	4.81	0.0531	Not significant
X_1X_3	2.81	1	2.81	7.48	0.0210	significant
X_2X_3	2.25	1	2.25	5.98	0.0345	significant
X_1^2	1736.86	1	1736.86	4623.79	< 0.0001	significant
X_2^2	3.636E-005	1	3.636E-005	9.681E-005	0.9923	Not significant

X_3^3	0.48	1	0.48	1.27	0.2862	Not significant
Residual	3.76	10	0.38	_	_	
Lack of Fit	2.78	5	0.56	2.86	0.1368	Not significant
Pure Error	0.97	5	0.19	_	_	
Cor Total	3960.37	19	_	_	_	
R-Squares	0.9991					
(c) Turbidity removal						
Model	1938.68	9	215.41	361.26	< 0.0001	significant
X_1	37.09	1	37.09	62.21	< 0.0001	significant
X_2	120.90	1	120.90	202.75	< 0.0001	significant
X_3	197.85	1	197.85	331.81	< 0.0001	significant
X_1X_2	0.015	1	0.015	0.026	0.8759	Not significant
X_1X_3	0.37	1	0.37	0.63	0.4467	Not significant
X_2X_3	6.94	1	6.94	11.64	0.0066	significant
X_1^2	816.49	1	816.49	1369.33	< 0.0001	significant
X_2^2	3.12	1	3.12	5.24	0.0451	Significant
X_3^3	0.14	1	0.14	0.24	0.6333	Not significant
Residual	5.96	10	0.60	_	_	
Lack of Fit	3.80	5	0.76	1.75	0.2762	Not significant
Pure Error	2.17	5	0.43	_	_	
Cor Total	1944.64	19	_	_	_	
R-Squares	0.9969					

3.3. Effects of operation parameters on COD removal efficiency

pH, contact time and adsorbent (Fe_3O_4/mordenite zeolite) amount had significant effects on COD removal according to the results in **Table 4(a)**. pH had the highest F-value of 837.51 hence is most significant effect on COD removal (Y_1) among the studied factors. The second effective studied factor on COD removal is Fe_3O_4/mordenite zeolite amount (X_3) with F-value of 360.75, while contact time (X_2) showed a less remarkable effect with F-value of 86.35. On the other hand, the interaction between pH and Fe_3O_4/mordenite zeolite amount (X_1X_3) had considerable effect on COD removal due to its F-value of 11.34 compared with less notable effect of interaction between contact time and Fe_3O_4/mordenite zeolite amount (X_2X_3). The

quadratic function of pH with F-value of 2659.45 showed significant effects on COD removal in comparison with the other parameters. 3D diagrams have been applied to show the effect of interaction of three parameters on COD, BOD and turbidity removal. **Figure 7(a-c)** show the effect of interaction between the studied variables on the COD removal.

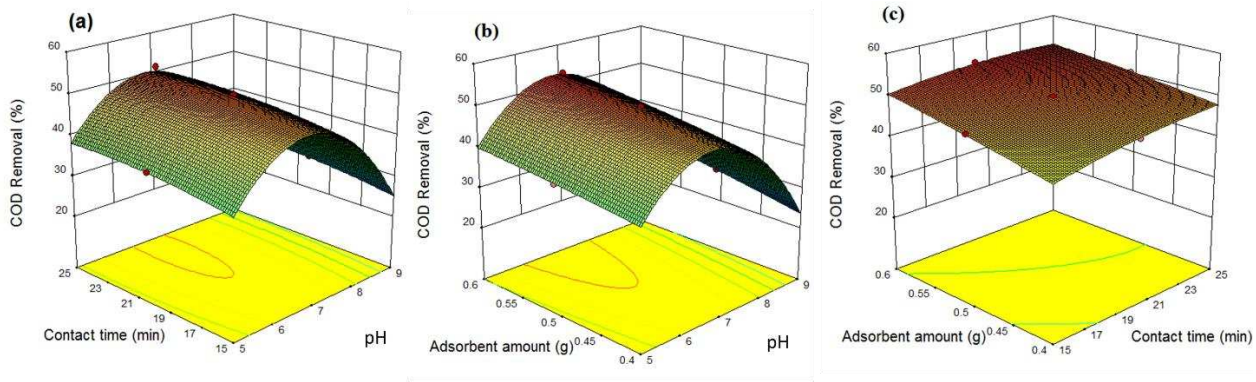

Figure 7. The 3D diagram of the effect of **(a)** pH and contact time **(b)** pH and adsorbent (Fe_3O_4/mordenite zeolite) amount **(c)** contact time and adsorbent (Fe_3O_4/mordenite zeolite) amount on the COD removal.

pH is reported to be one of the important parameters in wastewater treatment system [55]. The charge of the sorbent and sorbate is changed by the solution pH, and that can affect their electrostatic interaction. With an increasing pH, the surface charge becomes more negative ($^-$OH), whereas a lower pH value causes an increase of H^+ ions [56]. According to **Table 4(a)** the interaction between pH and contact time is not significant and the interaction between pH and Fe_3O_4/mordenite zeolite amount with p-value close to 0.05 also shows insignificant effect on COD removal. The insignificant interactions of X_1X_2 and X_1X_3 are also shown by 3D plots (**Figure 7a and 7b)**. According to the **Figure 7(a)**, at lower pH levels, by increasing the contact time the COD removal has no appreciable changes indicating to an insignificant interaction between these two parameters. On the other hand, by increasing the pH up to neutral the COD removal increased to highest value and then decreased by a further increase of pH. The interaction between pH and Fe_3O_4/mordenite zeolite amount on COD removal efficiency is shown in **Figure 7(b)**. It can be noticed that at pH<7, the COD removal does not significantly increase by increasing the amount of Fe_3O_4/mordenite zeolite. This could be ascribed to the partial destruction of zeolite framework at lower pH value [57]. **Figure 7(c)** shows the interaction effects between contact time and Fe_3O_4/mordenite zeolite amount. The results show

that the COD removal is at its lowest at lower contact time and Fe_3O_4/mordenite zeolite amount. By increasing both contact time and Fe_3O_4/mordenite zeolite amount, COD removal shows a significant increase and reaches the highest level at the maximum Fe_3O_4/mordenite zeolite amount (0.6 g) and contact time of 20 min. However, by increasing the contact time up to 25 min the COD removal rate slightly decreases. This can be explained by the fact that the Fe_3O_4/mordenite zeolite surface gets close to the saturation at longer contact time resulting in the slowdown in adsorption rate due to an increase in occupied pores [58].

3.4. Effects of operation parameters on BOD removal efficiency

The results of BOD removal in **Table 4(b)** indicate that all three variables have significant effects on BOD removal, where pH had the highest effect. The interaction effects between X_1X_3 and X_2X_3 are significant, where the interaction between pH and contact time with p-value > 0.05 does not show a significant effect on BOD removal. Moreover, only the quadratic effect of pH is considerable and X_2^2, X_3^2 showed no significant effects (the p-value > 0.05). The 3D response surface in Figure 8 (a-c) demonstrate the effects of the three parameters on BOD removal (Y_2). The 3D plot in **Figure 8(a)** shows the effect of interaction of pH and contact time on BOD removal where no significant interaction can be seen. The BOD removal, however, increases by enhancing the pH from acidic to 7 and then reduces with the further increase of pH. According to **Figure 8(b)**, a simultaneous increase in pH and Fe_3O_4/mordenite zeolite adsorbent amount, up to pH=7 and Fe_3O_4/mordenite zeolite amount 0.6 g, BOD increases to the maximum value (74.13) and after that the removal decreases. The interaction between adsorbent amount and contact time is shown in **Figure 8(c)**. According to this 3D plot, BOD removal increases continuously to the optimum amount of 80.12, where the contact time is 20 min and the amount of Fe_3O_4/mordenite zeolite is 0.6 g.

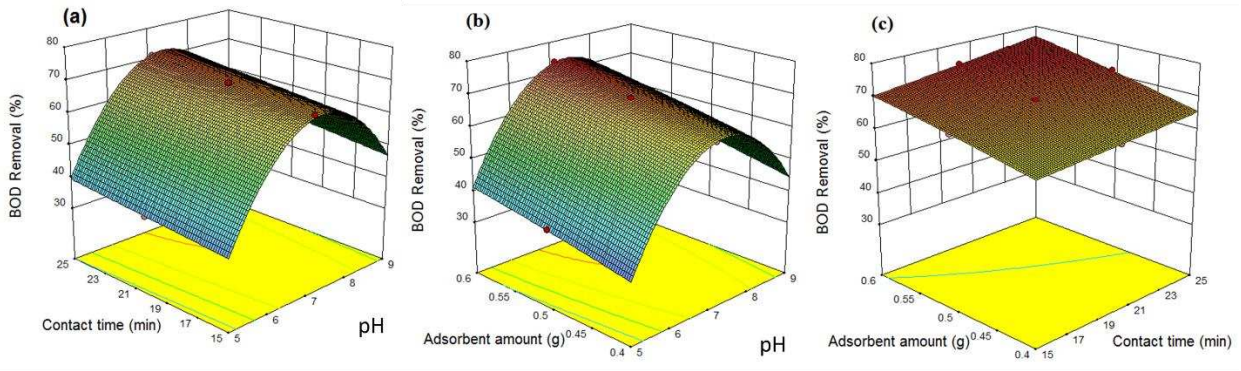

Figure 8. The 3D response surfaces for the effect of **(a)** pH and contact time **(b)** pH and adsorbent (Fe_3O_4/mordenite zeolite) amount **(c)** contact time and adsorbent (Fe_3O_4/mordenite zeolite) amount on the BOD removal.

3.5. Effects of operation parameters on Turbidity removal efficiency

According to **Table 4(c)**, all three parameters exhibit significant effects on turbidity removal. The interaction effects between pH and contact time (X_1X_3) and pH and Fe_3O_4/mordenite zeolite amount (X_1X_3) are not significant as the p-values are higher than 0.05. The interaction between contact time and Fe_3O_4/mordenite zeolite amount illustrates significant effects on turbidity removal. The quadratic effect of pH and contact time was significant, while it was not the case for the Fe_3O_4/mordenite zeolite amount. **Figure 9 (a-c)** demonstrates the 3D response surface for the effect of the variable parameters on the turbidity removal capacity (Y_3). The changes in contact time and Fe_3O_4/mordenite zeolite amount have no remarkable effect on turbidity removal at lower pH values [**Figure 9 (a & b)**]. By increasing the pH level to neutral the turbidity removal increases to 80.12 % at 20 min contact time in **Figure 9(a)** and 79.02% for Fe_3O_4/mordenite zeolite amount of 0.5 g in **Figure 9(b)**. By further increasing pH to 9 the turbidity removal capacity showed a decrease as shown in **Figure 9 (a & b)**. **Figure 9(c)** demonstrates the 3D response surface of contact time and absorbent amount. As can be seen, turbidity removal is the lowest (48.78%) at lower contact times and absorbent amounts, while it reaches a maximum at higher contact times.

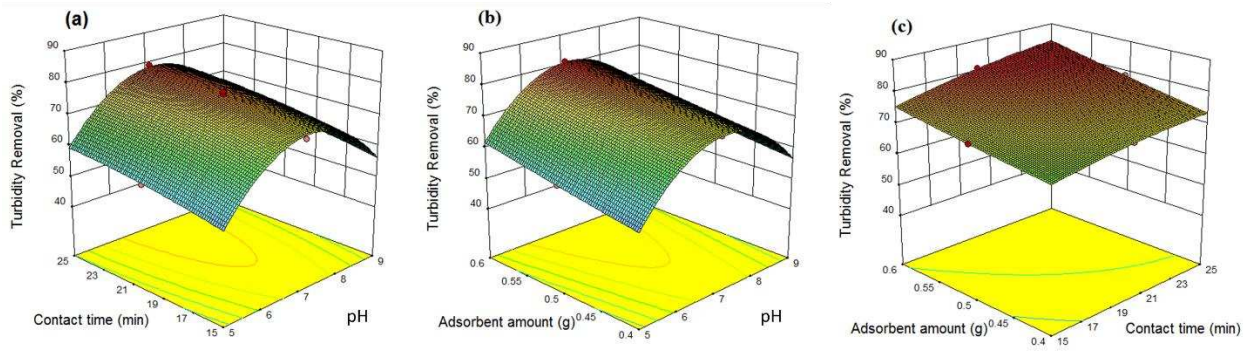

Figure 9. The 3D response surfaces for the effect of **(a)** pH and contact time **(b)** pH and adsorbent (Fe_3O_4/mordenite zeolite) amount **(c)** contact time and adsorbent (Fe_3O_4/mordenite zeolite) amount on the turbidity removal.

3.6. Reusability of Fe_3O_4/mordenite zeolite

The reusability of Fe_3O_4/mordenite zeolite through regeneration in a continuous process is very important since it determines the economics of the process [59]. The lifetime of Fe_3O_4/mordenite zeolite for COD, BOD and turbidity removal was studied by conducting five consecutive cycles of adsorption-desorption (**Figure 10**). The results show that the removal capacities of synthesised Fe_3O_4/mordenite zeolite for COD, BOD and turbidity removal decreased by about 17.36%, 18.36% and 20.34%, respectively, after five consecutive cycles. Thus, Fe_3O_4/mordenite zeolite has an excellent reusability and has good potential for an economic wastewater treatment in oil refineries.

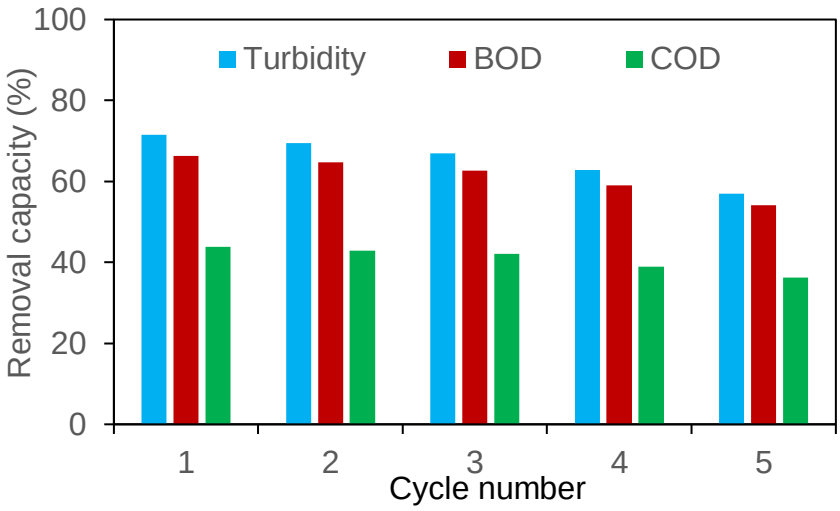

Figure 10. Reusability of Fe_3O_4/mordenite zeolite for COD, BOD and turbidity removal [pH of 7.81, contact time of 15.83 min, adsorbent (Fe_3O_4/mordenite zeolite) amount of 0.52 g].

3.7. Discussion

From economic point of view for an industrial application surface coated zeolite absorbent should be used with the highest removal efficiency. The Design Expert® software was implemented to optimise variable parameters for the removal capacity of COD, BOD and turbidity of Kermanshah oil refinery wastewaters. The optimum predicted conditions were pH of 7.81, contact time of 15.83 min, Fe_3O_4/mordenite zeolite amount of 0.52 g (in 100 g sample), with the COD removal of 43.78%, BOD removal of 66.33% and Turbidity removal of 71.45%. From experimental observation, the actual removal amount of COD, BOD and turbidity removal were 42.63%, 65.28% and 70.39%, respectively, under predicted optimum conditions of pH, contact time and Fe_3O_4/mordenite zeolite amount. The relative error for COD, BOD and turbidity removal was found to be 2.69%, 1.60% and 1.50%, respectively, suggesting that the present process optimisation method has a reasonable accuracy. It was also found that the iron oxide modification of mordenite zeolite led to stabilise the activity and reusability of synthesised Fe_3O_4/mordenite zeolite.

It is interesting to note that pH has the highest influence on the removal efficiency with the peak at near pH neutral. According to the literature, zeolite particles have a high sorption capacity for many different ions in wastewater solutions and the surface complexation mechanism is dominated. The surface complexation mechanism as well as surface precipitation are highly pH dependent. In current study as the pollutant are mainly organic and oily base, pH neutral would favour the adsorption process unlike the case for ionic pollutants. Hence the possible removal mechanism could be floating of zeolite with oil after contacting at specific time and neutral pH (Scheme 1). To fully verify this claim, the underlying adsorption mechanisms and its kinetics should however be studied in detail and this would be the subject of future studies.

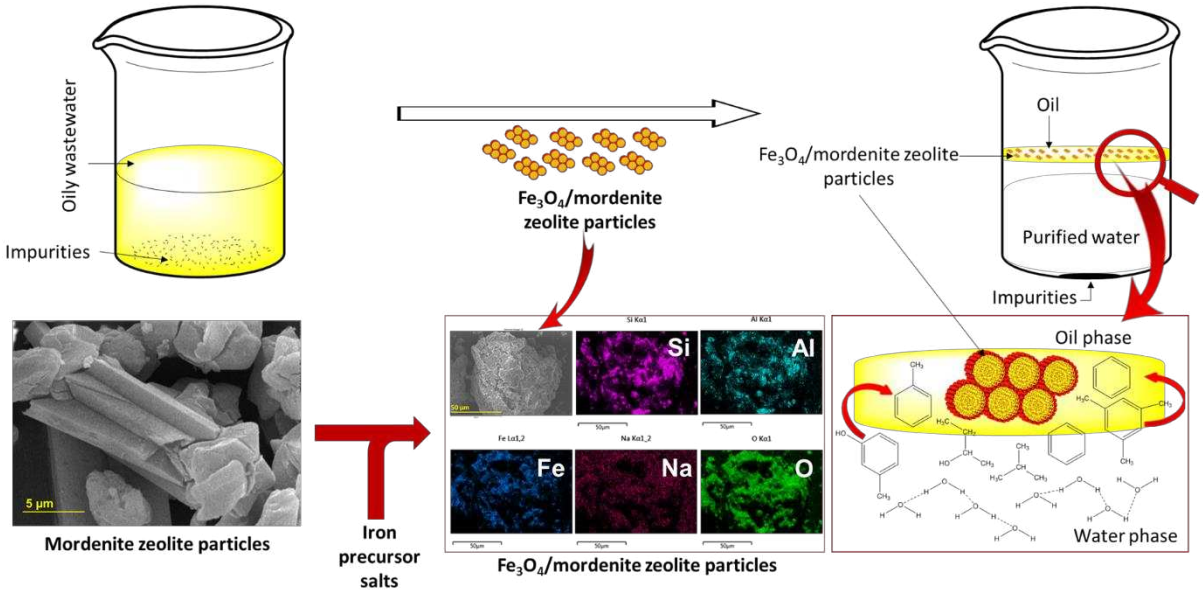

Scheme 1. Mechanism of oily wastewater purification over Fe_3O_4/mordenite zeolite

4. Conclusions

In this study, the response surface technique is implemented to optimise the removal parameters for oil refinery wastewater purification using Fe_3O_4/mordenite zeolite. The central composite design was carried out to investigate the effects of three variables of pH, contact time and Fe_3O_4/mordenite zeolite amount on the COD, BOD and turbidity removal capacity of Fe_3O_4/mordenite zeolite. The results indicated by increasing pH from acidic to neutral, the removal capacity increased to the maximum and further increasing pH caused a rapid decrease of removal of COD, BOD and turbidity removal. Based on the results it was found that pH was the most significant factor on COD and BOD removal capacity, whereas Fe_3O_4/mordenite zeolite amount was the most effective factor on turbidity removal capacity. Through process optimisation, the experimental results of COD, BOD and turbidity removal reasonably agree with the predicted values. The optimum conditions for removal capacity of Fe_3O_4/mordenite zeolite have been identified as a pH of 7.81, contact time of 5.83 min and amount of Fe_3O_4/mordenite zeolite of 0.52 g (in 100 g sample). The present study showed the prepared Fe_3O_4/mordenite zeolite could be reused for five consecutive cycles and can be applied in purification of wastewater treatment in oil refineries.

Acknowledgements

This work was supported by the Iran National Science Foundation (INSF, Grant Number: 95004135).

References

1. Wang, D., E. McLaughlin, R. Pfeffer, and Y.S. Lin, Adsorption of oils from pure liquid and oil–water emulsion on hydrophobic silica aerogels. Separation and Purification Technology, **2012**. 99: p. 28-35.
2. Núñez-Delgado, A., P. Sueiro-Blanco, S.S. Labandeira, and R.C. Torrijos, Polycyclic aromatic hydrocarbons concentrations in a waste from fuel oil spill and its mixture with other materials: Time-course evolution. Journal of Cleaner Production, **2018**. 172: p. 1910-1917.
3. Moslehyani, A., A. Ismail, M. Othman, and T. Matsuura, Design and performance study of hybrid photocatalytic reactor-PVDF/MWCNT nanocomposite membrane system for treatment of petroleum refinery wastewater. Desalination, **2015**. 363: p. 99-111.
4. Sun, Y., C. Zhu, H. Zheng, W. Sun, Y. Xu, X. Xiao, Z. You, and C. Liu, Characterization and coagulation behavior of polymeric aluminum ferric silicate for high-concentration oily wastewater treatment. Chemical Engineering Research and Design, **2017**. 119: p. 23-32.
5. Sarfaraz, M.V., E. Ahmadpour, A. Salahi, F. Rekabdar, and B. Mirza, Experimental investigation and modeling hybrid nano-porous membrane process for industrial oily wastewater treatment. Chemical Engineering Research and Design, **2012**. 90(10): p. 1642-1651.
6. Yu, L., M. Han, and F. He, A review of treating oily wastewater. Arabian journal of chemistry, **2017**. 10: p. S1913-S1922.
7. Jamaly, S., A. Giwa, and S.W. Hasan, Recent improvements in oily wastewater treatment: Progress, challenges, and future opportunities. Journal of Environmental Sciences, **2015**. 37: p. 15-30.
8. Diya'uddeen, B.H., W.M.A.W. Daud, and A.R. Abdul Aziz, Treatment technologies for petroleum refinery effluents: A review. Process Safety and Environmental Protection, **2011**. 89(2): p. 95-105.
9. El-Naas, M.H., M.A. Alhaija, and S. Al-Zuhair, Evaluation of a three-step process for the treatment of petroleum refinery wastewater. Journal of Environmental Chemical Engineering, **2014**. 2(1): p. 56-62.
10. Ma, R., J. Zhu, B. Wu, and X. Li, Adsorptive removal of organic chloride from model jet fuel by Na-LSX zeolite: Kinetic, equilibrium and thermodynamic studies. Chemical Engineering Research and Design, **2016**. 114: p. 321-330.
11. Visa, M., Synthesis and characterization of new zeolite materials obtained from fly ash for heavy metals removal in advanced wastewater treatment. Powder Technology, **2016**. 294: p. 338-347.
12. Wang, H., K.-Y. Lin, B. Jing, G. Krylova, G.E. Sigmon, P. McGinn, Y. Zhu, and C. Na, Removal of oil droplets from contaminated water using magnetic carbon nanotubes. Water research, **2013**. 47(12): p. 4198-4205.
13. Salam, M.A. and R.M. Mohamed, Removal of antimony (III) by multi-walled carbon nanotubes from model solution and environmental samples. Chemical Engineering Research and Design, **2013**. 91(7): p. 1352-1360.

14. Ahmadzadeh Tofighy, M. and T. Mohammadi, Nitrate removal from water using functionalized carbon nanotube sheets. Chemical Engineering Research and Design, **2012**. 90(11): p. 1815-1822.
15. Moazed, H. and T. Viraraghavan, Use of organo-clay/anthracite mixture in the separation of oil from oily waters. Energy sources, **2005**. 27(1-2): p. 101-112.
16. Rajakovic, V., G. Aleksic, M. Radetic, and L. Rajakovic, Efficiency of oil removal from real wastewater with different sorbent materials. Journal of hazardous materials, **2007**. 143(1): p. 494-499.
17. Moazed, H. and T. Viraraghavan, Removal of oil from water by bentonite organoclay. Practice Periodical of Hazardous, Toxic, and Radioactive Waste Management, **2005**. 9(2): p. 130-134.
18. Lin, K.-Y.A., H. Yang, C. Petit, and S.-Y. Chen, Removal of oil droplets from water using carbonized rice husk: enhancement by surface modification using polyethylenimine. Environmental Science and Pollution Research, **2015**. 22(11): p. 8316-8328.
19. Katal, R., M.S. Baei, H.T. Rahmati, and H. Esfandian, Kinetic, isotherm and thermodynamic study of nitrate adsorption from aqueous solution using modified rice husk. Journal of Industrial and Engineering Chemistry, **2012**. 18(1): p. 295-302.
20. Lin, K.-Y.A. and S.-Y. Chen, Enhanced removal of oil droplets from oil-in-water emulsions using polyethylenimine-modified rice husk. Waste and Biomass Valorization, **2015**. 6(4): p. 495-505.
21. Aly, A.A., Y.N. Hasan, and A.S. Al-Farraj, Olive mill wastewater treatment using a simple zeolite-based low-cost method. Journal of environmental management, **2014**. 145: p. 341-348.
22. Maruyama, H., H. Seki, and Y. Satoh, Removal kinetic model of oil droplet from o/w emulsion by adding methylated milk casein in flotation. Water research, **2012**. 46(9): p. 3094-3100.
23. Santo, C.E., V.J. Vilar, C.M. Botelho, A. Bhatnagar, E. Kumar, and R.A. Boaventura, Optimization of coagulation–flocculation and flotation parameters for the treatment of a petroleum refinery effluent from a Portuguese plant. Chemical Engineering Journal, **2012**. 183: p. 117-123.
24. Fan, Y., S. Simon, and J. Sjöblom, Chemical destabilization of crude oil emulsions: effect of nonionic surfactants as emulsion inhibitors. Energy & Fuels, **2009**. 23(9): p. 4575-4583.
25. Obaid, M., E. Yang, D.-H. Kang, M.-H. Yoon, and I.S. Kim, Underwater superoleophobic modified polysulfone electrospun membrane with efficient antifouling for ultrafast gravitational oil-water separation. Separation and Purification Technology, **2018**. 200: p. 284-293.
26. Wang, J., L.a. Hou, K. Yan, L. Zhang, and Q.J. Yu, Polydopamine nanocluster decorated electrospun nanofibrous membrane for separation of oil/water emulsions. Journal of Membrane Science, **2018**. 547: p. 156-162.
27. dos Santos Barbosa, A., A. dos Santos Barbosa, T.L.A. Barbosa, and M.G. Rodrigues, Synthesis of zeolite membrane (NaY/alumina): Effect of precursor of ceramic support and its application in the process of oil–water separation. Separation and Purification Technology, **2018**. 200: p. 141-154.
28. Gobbi, L.C., I.L. Nascimento, E.P. Muniz, S.M. Rocha, and P.S. Porto, Electrocoagulation with polarity switch for fast oil removal from oil in water emulsions. Journal of environmental management, **2018**. 213: p. 119-125.
29. Flores, N., E. Brillas, F. Centellas, R.M. Rodríguez, P.L. Cabot, J.A. Garrido, and I. Sirés, Treatment of olive oil mill wastewater by single electrocoagulation with different electrodes and sequential electrocoagulation/electrochemical Fenton-based processes. Journal of hazardous materials, **2018**. 347: p. 58-66.

30. Llamas, S., E. Santini, L. Liggieri, F. Salerni, D. Orsi, L. Cristofolini, and F. Ravera, Adsorption of sodium dodecyl sulfate at water–dodecane interface in relation to the oil in water emulsion properties. Langmuir, **2018**. 34(21): p. 5978-5989.
31. Elanchezhiyan, S.S., S.M. Prabhu, and S. Meenakshi, Effective adsorption of oil droplets from oil-in-water emulsion using metal ions encapsulated biopolymers: Role of metal ions and their mechanism in oil removal. International journal of biological macromolecules, **2018**. 112: p. 294-305.
32. Kundu, P. and I.M. Mishra, Removal of emulsified oil from oily wastewater (oil-in-water emulsion) using packed bed of polymeric resin beads. Separation and Purification Technology, **2013**. 118: p. 519-529.
33. Rashed, M.N., Adsorption technique for the removal of organic pollutants from water and wastewater. **2013**: INTECH Open Access Publisher.
34. Wang, J., Y. Zheng, and A. Wang, Coated kapok fiber for removal of spilled oil. Marine pollution bulletin, **2013**. 69(1): p. 91-96.
35. Mirshafiee, A., A. Rezaee, and R.S. Mamoori, A clean production process for edible oil removal from wastewater using an electroflotation with horizontal arrangement of mesh electrodes. Journal of Cleaner Production, **2018**.
36. Tan, Y.-X., Y.-P. He, M. Wang, and J. Zhang, A water-stable zeolite-like metal–organic framework for selective separation of organic dyes. RSC Advances, **2014**. 4(3): p. 1480-1483.
37. Lad, J.B. and Y.T. Makkawi, Adsorption of dimethyl ether (DME) on zeolite molecular sieves. Chemical Engineering Journal, **2014**. 256: p. 335-346.
38. Almasoudi, A. and R. Mokaya, A CVD route for the preparation of templated and activated carbons for gas storage applications using zeolitic imidazolate frameworks (ZIFs) as template. Microporous and Mesoporous Materials, **2014**. 195: p. 258-265.
39. Fegade, S.L., *Retraction notice to "Aromatics from 1*-tetradecene through conversion over *zeolite catalysts" Chem. Eng. Res. Des. 113 (2016) 182*–188. Chemical Engineering Research and Design, **2017**. 120: p. 423.
40. Nizami, A., O. Ouda, M. Rehan, A. El-Maghraby, J. Gardy, A. Hassanpour, S. Kumar, and I. Ismail, The potential of Saudi Arabian natural zeolites in energy recovery technologies. Energy, **2016**. 108: p. 162-171.
41. Rehan, M., R. Miandad, M. Barakat, I. Ismail, T. Almeelbi, J. Gardy, A. Hassanpour, M. Khan, A. Demirbas, and A. Nizami, Effect of zeolite catalysts on pyrolysis liquid oil. International Biodeterioration & Biodegradation, **2017**. 119: p. 162-175.
42. Miandad, R., M. Barakat, M. Rehan, A. Aburiazaiza, J. Gardy, and A. Nizami, Effect of advanced catalysts on tire waste pyrolysis oil. Process Safety and Environmental Protection, **2018**. 116: p. 542-552.
43. Molla, A., Z. Ioannou, A. Dimirkou, and K. Skordas, Surfactant modified zeolites with iron oxide for the removal of ammonium and nitrate ions from waters and soils. Topics in Chemistry and Material Science, **2014**. 7: p. 38-49.
44. Keshavarzi, N., F. Mashayekhy Rad, A. Mace, F. Ansari, F. Akhtar, U. Nilsson, L. Berglund, and L. Bergström, Nanocellulose–Zeolite Composite Films for Odor Elimination. ACS applied materials & interfaces, **2015**. 7(26): p. 14254-14262.
45. Hernández-Montoya, V., M.A. Pérez-Cruz, D.I. Mendoza-Castillo, M. Moreno-Virgen, and A. Bonilla-Petriciolet, Competitive adsorption of dyes and heavy metals on zeolitic structures. Journal of environmental management, **2013**. 116: p. 213-221.
46. Lv, G., Z. Li, W.-T. Jiang, C. Ackley, N. Fenske, and N. Demarco, Removal of Cr(VI) from water using Fe(II)-modified natural zeolite. Chemical Engineering Research and Design, **2014**. 92(2): p. 384-390.

47. Panwar, V., P. Kumar, A. Bansal, S.S. Ray, and S.L. Jain, PEGylated magnetic nanoparticles (PEG@ Fe_3O_4) as cost effective alternative for oxidative cyanation of tertiary amines via CH activation. Applied Catalysis A: General, **2015**. 498: p. 25-31.
48. Gardy, J., A. Osatiashtiani, O. Céspedes, A. Hassanpour, X. Lai, A.F. Lee, K. Wilson, and M. Rehan, A magnetically separable SO_4/Fe-Al-TiO_2 solid acid catalyst for biodiesel production from waste cooking oil. Applied Catalysis B: Environmental, **2018**.
49. Ali, M.M.M. and M.J. Ahmed, Adsorption behavior of doxycycline antibiotic on NaY zeolite from wheat (Triticum aestivum) straws ash. Journal of the Taiwan Institute of Chemical Engineers, **2017**. 81: p. 218-224.
50. Hesas, R.H., A. Arami-Niya, W.M.A.W. Daud, and J. Sahu, Preparation of granular activated carbon from oil palm shell by microwave-induced chemical activation: Optimisation using surface response methodology. Chemical Engineering Research and Design, **2013**. 91(12): p. 2447-2456.
51. Montgomery, D.C., Design and Analysis of Experiments, **2001**. 5th Ed., John Wiley and Sons Inc., New York.
52. Khanday, W.A., S.A. Majid, S.C. Shekar, and R. Tomar, Synthesis and characterization of various zeolites and study of dynamic adsorption of dimethyl methyl phosphate over them. Materials Research Bulletin, **2013**. 48(11): p. 4679-4686.
53. Khanday, W., F. Marrakchi, M. Asif, and B. Hameed, Mesoporous zeolite–activated carbon composite from oil palm ash as an effective adsorbent for methylene blue. Journal of the Taiwan Institute of Chemical Engineers, **2017**. 70: p. 32-41.
54. Klobes, P., K. Meyer, and R.G. Munro, Porosity and specific surface area measurements for solid materials. **2006**.
55. Baei, M.S., H. Esfandian, and A.A. Nesheli, Removal of nitrate from aqueous solutions in batch systems using activated perlite: an application of response surface methodology. Asia-Pacific Journal of Chemical Engineering, **2016**. 11(3): p. 437-447.
56. Hongxia, Z., W. Xiaoyun, L. Honghong, T. Tianshe, and W. Wangsuo, Adsorption behavior of Th(IV) onto illite: Effect of contact time, pH value, ionic strength, humic acid and temperature. Applied Clay Science, **2016**. 127–128: p. 35-43.
57. Mehdizadeh, S., S. Sadjadi, S.J. Ahmadi, and M. Outokesh, Removal of heavy metals from aqueous solution using platinum nanopartcles/Zeolite-4A. Journal of Environmental Health Science and Engineering, **2014**. 12(1): p. 7.
58. Ravanan, M., M. Ghaedi, A. Ansari, F. Taghizadeh, and D. Elhamifar, Comparison of the efficiency of Cu and silver nanoparticle loaded on supports for the removal of Eosin Y from aqueous solution: Kinetic and isotherm study. Spectrochimica Acta Part A: Molecular and Biomolecular Spectroscopy, **2014**. 123: p. 467-472.
59. Lye, J.W.P., N. Saman, S.S.N. Sharuddin, N.S. Othman, S.S. Mohtar, A.M.M. Noor, J. Buhari, S.C. Cheu, H. Kong, and H. Mat, Removal performance of tetracycline and oxytetracycline from aqueous solution via natural zeolites: An equilibrium and kinetic study. CLEAN–Soil, Air, Water, **2017**.